Available online at www.sciencedirect.com

ScienceDirect

Procedia Structural Integrity 39 (2022) 104–110

Structural Integrity Procedia

www.elsevier.com/locate/procedia

7th International Conference on Crack Paths

Rolling effect in fretting fatigue test at the crack initiation stage

Diego Erena [a]*, Vicente Martín [a], Jesús Vázquez [a], Carlos Navarro [a]

[a] *Departamento de Ingeniería Mecánica y Fabricación, Universidad de Sevilla, Camino de los descubrimientos s/n, 41092 Sevilla*

Abstract

The aim of this work is to perform a detailed analysis of the cracks paths obtained in fretting fatigue tests with cylindrical contact but taking into account the presence of an unavoidable (due to the fretting device's stiffness) small oscillatory rolling. In order to obtain the crack paths crack surfaces were measured with a confocal microscope after the tests. Besides, the contact area and the surface crack initiation location were obtained by means of an optical microscope. The measurements indicate that the contact area is substantially larger than the theoretical one according to Hertz´s theory, contrary to tests done with only static normal load, in which both theoretical and experimental areas match perfectly. This observation means, that, due to the surface contact pad's geometry (cylindrical) and the stiffness of the test setup, rolling is occurring during tests when tangential loading is developed. To reproduce this phenomenon, a 2D FEM model is developed. Stress/strain fields along the fretting cycle are analysed, noticing a substantial change of the contact surface hot-spot point and surface contact stress distribution, when compared with the non-rolling case. To predict the initial crack path, a previously developed model, based on a critical plane parameter, is applied using FEM stress/strain results. The results obtained show a better prediction of the surface hot-spot point and initial crack orientation estimation, when compared with the non-rolling case, and considering as a reference the experimental crack paths measured via confocal microscope.

Keywords: Fretting fatigue; Cylindrical contact; Numeric model

* Corresponding author. Tel.: +34954482178.
E-mail address: deg@us.es

10.1016/j.prostr.2022.03.078

1. Main text

Fretting fatigue is a material damage that appears in mechanical contacts. It is produced when a frictional contact pair is subjected to very small oscillatory relative displacements. The amplitude of those relative displacements is usually in the order of thousandths or hundredths of a millimetre. The normal and tangential loads between the mating surfaces usually produce a very high, and stepped, stress/strain field close to the contact edges that cyclically varies with the relative displacements. The varying of these stresses/strains initiate small surface cracks at the hot-spot zones that can grow through the zone where stresses are high enough. These relative displacements are generally produced by global loads or displacements applied to the elements in contact that also generate a global stress field in the components. If the global stress field is high enough, initiated cracks can continue growing until the complete fracture of the components. There are many examples of mechanical elements prone to fretting-fatigue failure, such as bolted or riveted joints, rotor-blade dovetail connections, metal cables, or shrink-fitted couplings.

Due to the presence of a tangential load, and considering the stiffness of the contact pair, in some practical cases a small rotation can be produced between the mating surfaces. The stiffness of the contact pair depends on the fretting fatigue bridges design. There are numerous designs of fretting fatigue bridges with different contact pair stiffness. Among them, the one designed by Wittkowsky and Dominguez (1999) that is used in our laboratory by several authors as Vázquez et al (2012) and most recently by Martín et al. (2020), will be studied.

2. Experimental campaign

In the current work a cylindrical contact pair is studied, in which a cylindrical contact pad of radius, R, is pressed against a flat surface. A scheme of the device used to conduct the fretting tests is shown in Fig.1a. This type of device has been used for large campaigns of cylindrical and spherical fretting fatigue tests during the last decades. In that test setup, initially the cylindrical contact pads are pressed against the flat surface of a dog-bone type fretting fatigue test specimen with a constant normal load, N. Then, a fully reversed cyclic axial load of amplitude, P_a, is applied directly to the specimen by means of a hydraulic actuator. Then, and due to the device's stiffness, an in-phase (with P_a) tangential load, Q, appears. The Q amplitude can be adjusted to the desired value, just moving the adjustable supports acting as a leaf springs (see Fig. 1a), and thus modifying device's stiffness. Main specimen and pad parameters are shown in Fig. 1b.

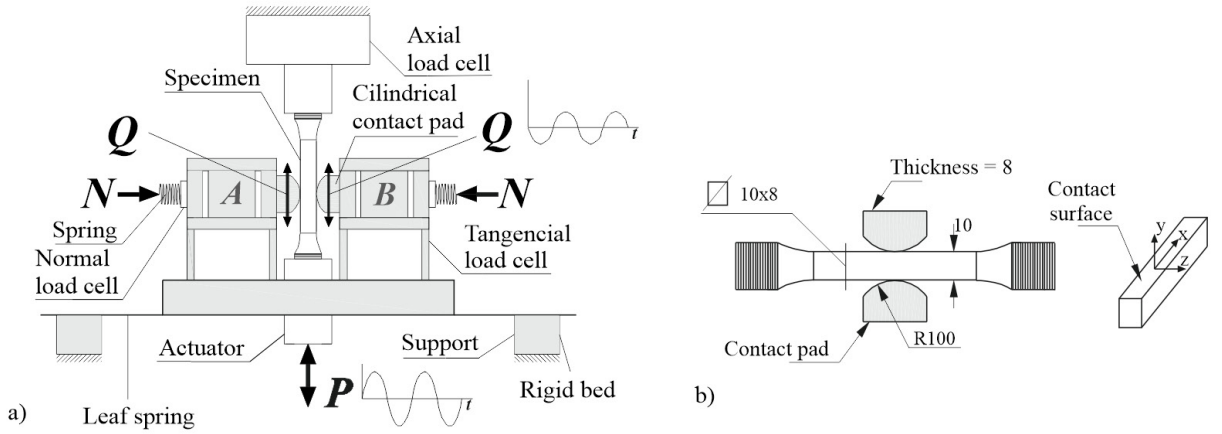

Fig. 1. (a) Scheme of the fretting fatigue device used in the experimental campaign; (b) main geometric characteristics –in mm- for the "dog bone" type fretting fatigue test specimens and contact pads.

Both contact pads and test specimens were made in aluminium alloy Al 7075-T651, which is widely used in the manufacture of aircraft components. The main mechanical properties for this material are shown in Table 1.

The three analysed tests studied are shown in Table 2, including the load values defining a cycle, the theoretical contact semi-width according to Hertz´s theory, a_H, the maximum contact pressure, p_0, and the range of the analytical axial stress at the contact trailing edge (x = a_H), $\Delta\sigma_{xx}$.

Table 1. Material properties Al 7075-T651.

Young's modulus, E	71 GPa
Poisson's ratio, υ	0.33
Yield strength, σ_y	503 MPa
Tensile strength, σ_y	572 MPa
Friction coefficient, μ	0.75

Table 2. Fretting fatigue loads and related Hertzian parameters for analysed tests

Test	N (N)	Q (N)	σ (MPa)	a_H (mm)	p_0 (MPa)	$\Delta\sigma_{xx}$ (x=a_H)
1	4217	1543	110	1.30	258.6	810.7
2	5429	971	150	1.47	293.4	1086.3
3	5429	1543	150	1.47	293.4	1026.3

Due to the fretting fatigue device's compliance and the contact geometry, small pad rotations are observed during tests. This preliminary observation gives rise to the study developed in this work. According to the Hertz´s theory the contact semi-width, a_H, depends exclusively on the normal load, material properties and pad radius, R (see Eq. 1). To confirm the theory some static tests were carried out to the cylindrical contact pair applying only a contact load N and measuring the obtained semi-width. Noticing that the theoretical semi-width agrees very well with the experimentally measured ones.

$$a_H = \sqrt{\frac{8NR(1-\nu^2)}{\pi E}} \tag{1}$$

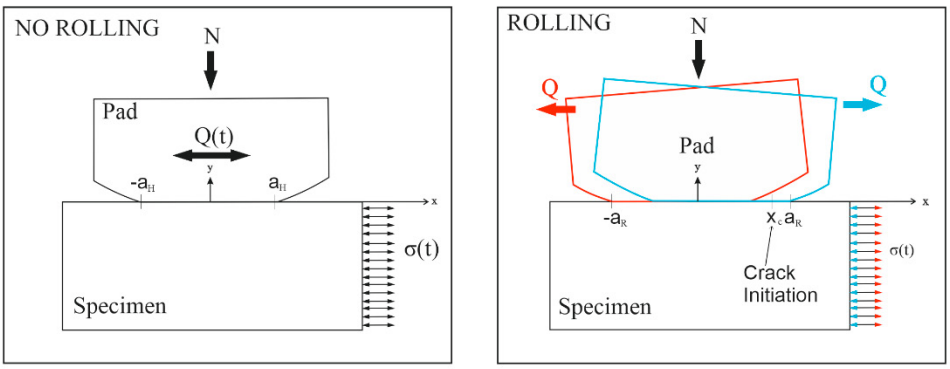

Fig. 2. (a) Scheme of the cylindrical contact without rolling; (b) Scheme of the cylindrical contact with rolling.

Table 3. Fretting fatigue rolling parameters

Test	a_R (mm)	a_H (mm)	$s = a_R - a_H$ (mm)	a_H (mm)	a_R/a_H	α=s/R (°)	x_c (mm)
1	1.64	1.30	0.34	1.30	1.26	0.19	1.41
2	1.74	1.47	0.27	1.47	1.18	0.15	1.54
3	1.80	1.47	0.33	1.47	1.26	0.19	1.48

Then, once the theory is validated, actual fretting scars produced during tests, were measured to obtain an average semi-width for each test, a_R. The theoretical and experimental semi-widths are compared in Table 3, corroborating that experimental scars are larger than the theoretical ones. Fig. 2 shows the movement of the pad and the meaning of the widths measured with and without rolling. In view of these results, it is possible to state that some rolling appears in the assembly, which could modify the performance of the tests as will be studied in the following sections. The extra contact semi-length due to rolling, *s,* could be obtained from the difference between the experimental semi-width, a_R, and the theoretical one, a_H, as shown in Table 3. Then, knowing *s*, that is the rolled arc length, and the pad's radius (R = 100 mm), the rotated angle by the pad, α, could be obtained (see Table 3). Besides, the crack initiation surface position is also measured, x_c, noticing that cracks initiates slightly inside of the actual contact zone and not at the contact trailing edge. All measurements have been made by means of images obtained from optical microscopes.

3. Numerical model

The aforementioned test configuration is modelled in ANSYS® software. Taking advantage of the symmetry of the test setup, only one of the two contact pair is modelled. Boundary conditions and most significant dimensions for that model are shown in Fig. 3a. To reproduce the test performance, loads are applied in six steps (see Fig. 3b). The first step applies the normal load, $N^*=N/t$ (t = 8mm), and it is kept constant during the remaining steps. The second step applies at the same time a tractive bulk stress, a tangential force to the left, $Q^*=Q/t$, and a counter clockwise rotation to the pad, α. The third step returns to the initial state, but maintaining the normal load. In the fourth state, loads are applied in the same manner as step 2 but in opposite directions. The step 5 returns to the state without loads and finally step 6 repeat loads from state 2. Global dimensions and relevant parameters of the model are shown in Fig.3a. Loads Q^* and N^* and the rotating angle α, are applied to a master node, located at the geometrical centre of the pad, that transfer these loads to all nodes lying on the top of the pad (see Fig. 3a). The rotation of the master node is restricted in the no-rolling cases.

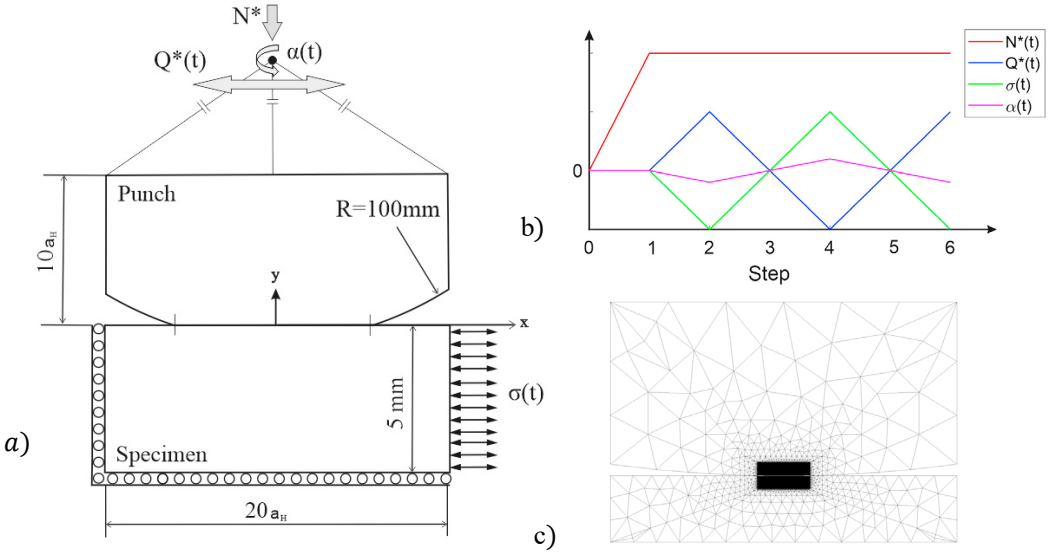

Fig. 3. (a) Scheme of the cylindrical contact and boundary conditions; (b) Loading steps; (c) Assembly mesh

The element type used for modelling the components is the PLANE182, which is a 2D plane element, with 2 degrees of freedom at each node, linear formulation, and 2 possible element shapes: triangular and quadrilateral. Due to the pads and test specimens' dimensions, it is suitable to use a plane strain formulation. The near contact zone is modelled with quadrilateral elements of 5 μm, while the rest of the model is meshed with triangular elements as can be seen in Fig. 3c. According to plane elements, elements CONTA171 and TARGE169 are used to model the contact pair. The contact formulation used is the augmented Lagrange method because of its well behaviour when friction is contemplated.

4. Results

Test from Table 2 are reproduced with the numerical model and the range of the surface direct stress between steps 4 and 6, $\Delta\sigma_{xx}$, is studied, considering that this is the parameter governing the crack initiation phenomenon. Although the fretting phenomena is strongly multiaxial, especially below the near contact surface material, the study of the $\Delta\sigma_{xx}$ surface stress is a good and easy approximation to the surface crack initiation process. The results obtained are shown in Fig. 4, comparing the cases with and without rolling. The axial stress range, $\Delta\sigma_{xx}$, is divided by the maximum contact pressure, p_0, according to Hertz´s theory. In addition, the surface longitudinal coordinate is divided by the theoretical contact Hertz semi-width, a_H. The graphs show two plotted lines; the black is the no-rolling case in which it can be seen that the hot spot is at the contact trailing edge, i.e. as the theory states. The green line represents the configuration with rolling, and in this case it cannot be said that there is a clear point of maximum values for the axial stress range, instead there is a zone (some kind of plateau) of high stress levels in which the values are almost constant. These preliminary numerical results are in very good agreement with the crack initiation surface coordinate position measured. Although simulations show that there is not a clear point for crack initiation, the maximum values are found in a range approximately between $0.8a_H$ and $1.2a_H$, values that are in line with experimental cracks which were observed inside this range and not at the contact edge as Hertz theory states. Moreover, as the trailing edge is not fixed in the case of rolling, it moves as the loads are applied, the maximum stress range is lower than the case without rolling. These preliminary results suggest that rolling should be taking into account when tests are carried out in laboratory conditions for some fretting machines that allow some pad rotations.

Fig. 4. (a) Scheme of the cylindrical contact and boundary conditions; (b) Loading steps; (c) Assembly mesh.

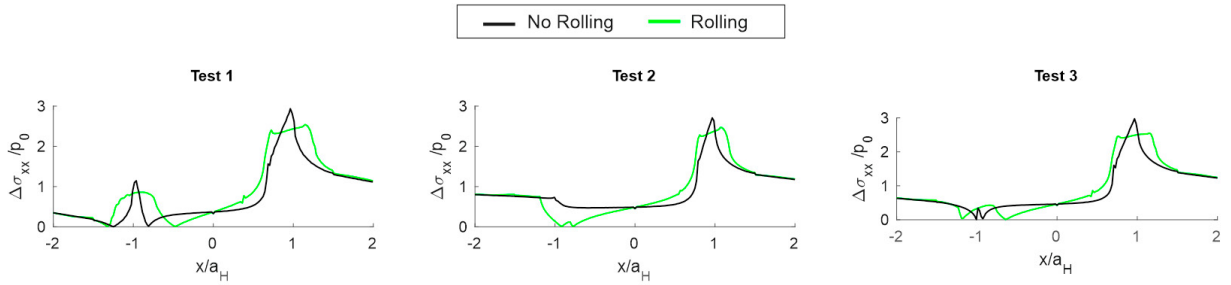

The influence of the rolling is also studied in the prediction of the initial crack path orientation. The procedure developed by Vázquez et al. (2017), and used in subsequent author works to predict the initial orientation of cracks emanating from the contact surface: Navarro et al. (2017) and Erena et al. (2018), is applied. In this procedure, first critical (hot-spot) points are defined for both cases: with and without rolling (see Fig.5a). The theoretical contact edge, x=a, is used as critical point for the no-rolling case and the crack initiation experimental position, x_c, for the rolling cases. Then, the multiaxial SWT parameter is calculated at discrete points along several lines (or material planes) ranging from θ=-90º to θ=90º and starting from the corresponding critical point (see Fig. 5a), but with the peculiarity that, for all of these points, the orientation for the material plane considered to evaluate the SWT parameter is not the critical one, but is that one coinciding with the orientation imposed by the θ angle. Then, the average value of the SWT parameter along each line is calculated, and the line having the highest mean value of the parameter is considered

to be the most likely to initiate a crack (see Fig. 5b). In the present work the material planes length is $r^* = 50$ μm, which is roughly the grain size for the Al7075-T651.

As can be seen in Fig 5b, in the case without rolling the maximum value of the parameter is found for an orientation of approximately 3º which means that predicted cracks without rolling are almost vertical. However, when the procedure is applied to the rolling case, the orientations are larger than the aforementioned case (≈10º), which is in more agreement with the results measured by the authors in former works as shown in the work of Vazquez et al. (2017).

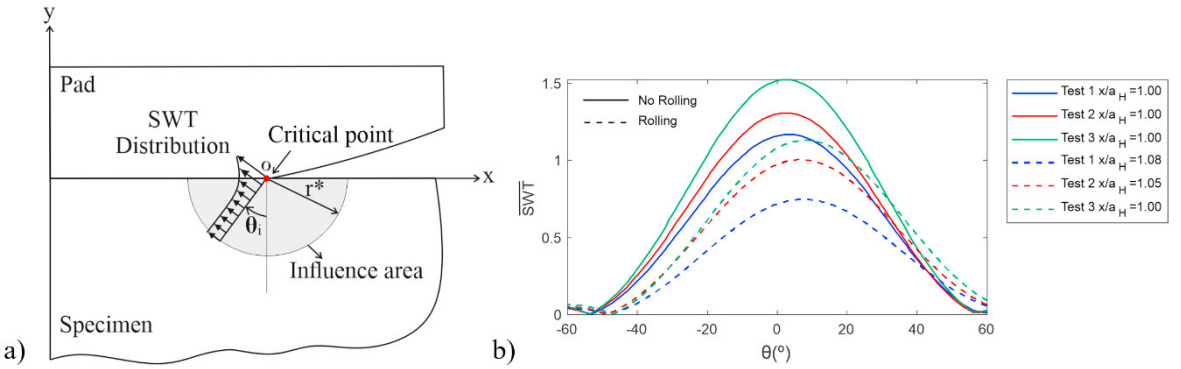

Fig. 5. (a) Crack initiation procedure; (b) Crack orientation results.

5. Conclusions

The first conclusion is that the fretting fatigue bridge produces an effect of rolling on the contact pads which increases the contact zones and this results in different contact surface stress and strain fields. It has been observed through the experimental measurements that the cracks initiations points do not appear at the contact trailing edge but within the contact zone, and this was verified by the FEM analysis. Finally, the crack initiation path has been predicted by means of the SWT multiaxial fatigue parameter, and these predicted paths have been compared with the experimental ones. By this comparison, it is possible to see that, if rolling is considered, better crack initiation paths are predicted if compared with the no-rolling case, corroborating thus the importance of the rolling effect in the fretting fatigue phenomenon.

Acknowledgements

The authors would like to thank the Fondo Europeo de Desarrollo Regional, Ministerio de Ciencia e Innovación and the Agencia Estatal de Investigación for the funding of the project RTI2018-09659-B-100.

References

Wittkowsky, B.U., Birch, J, Dominguez Abascal, J., Suresh, S., 1999. An Apparatus for Quantitative Fretting Fatigue Testing. Fatigue & Fracture of Engineering Materials & Structures. 22-4. Pp. 307-320.

Vázquez Valeo, Jesús, Navarro Pintado, Carlos, Dominguez Abascal, Jaime: Experimental results in fretting fatigue with shot and laser peened Al 7075-T651 specimens. En: International Journal of Fatigue. 2012. Vol. 40. Pag. 143-153. http://dx.doi.org/10.1016/j.ijfatigue.2011.12.014.

Martín, Vicente, Vázquez Valeo, Jesús, Navarro Pintado, Carlos, Dominguez Abascal, Jaime: Effect of shot peening residual stresses and surface roughness on fretting fatigue strength of Al 7075-T651. En: Tribology International. 2020. Vol. 142. Núm. 106004. 10.1016/j.triboint.2019.106004.

Vázquez J, Navarro C, Dominguez J. Analysis of fretting fatigue initial crack path in Al7075-T651 using cylindrical contact. Trib. Int. 2017;108:87-94.

Navarro, C., Vázquez, J., Domínguez, J. Nucleation and early crack path in fretting fatigue. Int. J. Fatigue. 2017:100:602–610. https://doi.org/10.1016/j.ijfatigue.2016.12.028

Erena, D., Vázquez, J., Navarro, C., Domínguez, J. Voids as stress relievers and a palliative in fretting. Fatigue Fract. Eng. Mater. Struct. 2018:41: 2475–2484. https://doi.org/10.1111/ffe.12849